water

Article

A Method for Calculating Water Demand for Sediment Transport Based on the Principles of River Dynamics

Lin Hou [1], Hongwu Zhang [1], Linqi Li [1,*], Junchi Zhao [2] and Xiji Li [3]

[1] Department of Hydraulics and Hydropower Engineering, Tsinghua University, Beijing 100084, China; houl20@mails.tsinghua.edu.cn (L.H.); zhhw@mail.tsinghua.edu.cn (H.Z.)
[2] Institute of Architecture Design and Research, Chinese Academy of Sciences, Beijing 100190, China
[3] Shandong Weifang Pumped Storage Co., Ltd., Weifang 261000, China
* Correspondence: lilq19@mails.tsinghua.edu.cn; Tel.: +86-13552333599

Abstract: Sufficient water is pivotal in maintaining the stability of boundaries in sandy river systems. However the current methodologies employed for computing the water demand for sediment transport in rivers frequently neglect this component. This research utilizes data spanning 1960 to 2020 from seven principal hydrological stations located in the lower Yellow River to establish the correlation between key factors pertaining to the sediment transport capacity of flow. A closed equation system was established based on the principles of river dynamics to solve unknown hydraulic parameters. Finding a suitable hydraulic geometric relationship equation as a supplementary equation is a key step in constructing a closed equation system. The findings indicate that sediment transport water demands are 71.79, 133.24, 226.89, 286.12, and 313.6 $\times$ 10^8 m^3, respectively, when sediment inflow is at 1, 2, 4, 6, and 8 $\times$ 10^8 t, with a bankfull discharge of 4000 m^3/s. As the sediment inflow diminishes and the unit water demand for sediment transport increases, the sediment transport efficiency of the lower Yellow River reduces. The outcomes of this research can serve as a foundation for the joint operation of the Yellow River's main and branch reservoirs, as well as for designing water resource allocation schemes within the basin.

Keywords: the lower Yellow River; river dynamics; hydraulic geometric relationship; bankfull discharge; sediment transport efficiency

Citation: Hou, L.; Zhang, H.; Li, L.; Zhao, J.; Li, X. A Method for Calculating Water Demand for Sediment Transport Based on the Principles of River Dynamics. *Water* **2023**, *15*, 3514. https://doi.org/10.3390/w15193514

Academic Editor: Bommanna Krishnappan

Received: 3 September 2023
Revised: 1 October 2023
Accepted: 3 October 2023
Published: 8 October 2023

1. Introduction

The multifunctional river system, encompassing elements such as water transportation, sediment transport, flood mitigation, profitability, navigation, and ecology, plays an essential role in our environment [1,2]. With the escalating pressure from various water resource and ecological challenges, there is an emerging scholarly consensus emphasizing that water resource management plans need to strike a balance between human water demand [3], ecological systems [4], and socio-economic development [5]. This approach places particular emphasis on ecological water and regional environmental flow [6,7]. The ecological water of a river refers to the volume of water necessary to sustain and protect specific ecological functions of a river without causing damage [8,9]. It is an important object of research on water resource management. Scholars have conducted extensive research on this issue [10–12]. However, they often neglect an essential component of ecological water demand in their research—the sediment transport water in sandy rivers [13].

In river systems characterized by high sediment concentrations, fulfilling the water demand for sediment transport is imperative to ensure the sediment is conveyed to the sea [14,15]. Failure to do so can result in significant sediment deposition, which can elevate the riverbed, thereby increasing flood risks and adversely affecting the ecological integrity of the river systems. In sandy river systems, providing adequate water for sediment transport prevents flooding by ensuring sufficient water volume for sediment transport, maintains the stability of the river system boundary, and facilitates the normal evolution of the river channel [16,17]. For rivers characterized by high sediment concentration, the formulation of appropriate release strategies can assist in reducing sediment deposition in reservoirs and downstream channels. Scholars have proposed varied definitions for sediment transport water demand, including unit water demand that reflects sediment transport efficiency [18,19], total water volume required to transport sediment without causing erosion or siltation, and water demand for sediment transport in plastic channels under bankfull beach flow and sediment inflow conditions [20]. These differing definitions contribute to variations in research methods and calculations for sediment transport water demand. In general, the amount of water required for sediment transport correlates with the conditions of incoming water and sediment, the desired control level of downstream river sedimentation, and the reservoir water and sediment regulation method. For natural alluvial rivers, the water and sediment in the basin are usually in a non-equilibrium state in spatio-temporal movement and evolution, and the river channel is in a constant equilibrium response process of erosion and sedimentation adjustment [21]. As a certain proportion of erosion and sedimentation should be allowed in the river channel, the sediment transport water demand calculated using river dynamics methods needs to be considered from the average scale of many years, with the erosion and sedimentation changes in an equilibrium state.

Renowned both domestically and globally, the Yellow River is a prominent example of a sandy river. Rapid elevation of the riverbed due to excessive sediment accumulation in the downstream channel can significantly amplify flood risks [22,23]. Consequently, it is essential to ensure sufficient water for sediment transport downstream of the Yellow River. Several scholars have conducted in-depth studies on this topic. For instance, Ni et al. [24] scrutinized the sediment transport water demand in the lower reaches of the Yellow River, offering a statistical minimum sediment transport water demand based on the river's high sediment concentration characteristics. Shen et al. [25], on the other hand, incorporated parameters of water and sediment allocation and the percentage of river sedimentation into his analysis. Utilizing measurement data, he formulated a calculation for the water demand for sediment transport during flood and peak seasons for the principal control stations in the lower Yellow River. This study quantified the impact of changes in water and sediment conditions and allowable sedimentation on the river's sediment transport water demand. Liu et al. [21] analyzed the variations and adjustable thresholds of sediment transport water consumption in different downstream river sections of the Yellow River, taking into account different inflow and sediment states and sediment transport objectives. However, a review of these findings reveals that the relationship between water demand for sediment transport and hydraulic sediment factors is mostly empirical and can only be applied to specific periods and river sections. Moreover, most of these calculation methods for sediment transport water only consider the impact of flow and sediment concentration, neglecting factors such as sediment hydraulic roughness and riverbed boundary. Therefore, establishing the structural relationship between sediment transport water consumption in river channels and ecological water under different spatio-temporal conditions is the critical next step in studying water demand for sediment transport in rivers [26,27].

Recent research results concerning sediment transport water in the lower Yellow River have been deemed unsuitable in light of the evolving water, sediment, and river channel conditions. Furthermore, upcoming reservoir water transfer plans for the Yellow River's main stream necessitate robust data support. This paper, from a balanced sediment transport viewpoint, postulates the concept of 'water demand for sediment transport'. This is defined as the volume of water needed to transport a specified amount of sediment within a distinct river stretch, assuming equilibrium under certain conditions of inflow water, sediment, and riverbed boundaries. This designated volume represents the mean annual water requirement to ensure that the main channel does not contract and that the riverbed does not become elevated, given an average sediment input anticipated for the coming years. Minor variations in riverbed erosion and sedimentation during the dry season are permissible. The objective of this study is to elucidate the primary hydraulic determinants that influence the usage of sediment transport water. Relying on river dynamics principles, an integrated equation system is devised. This system integrates the continuity equation, the motion equation, the movable bed resistance formula, and the hydraulic geometry relationship. Subsequently, these parameters are incorporated into the sediment transport equation to determine the equilibrium sediment concentration. This provides a methodology to compute the sediment transport water demand essential for maintaining the river's equilibrium state. A pivotal aspect of this system is identifying an appropriate hydraulic geometry relationship equation as an ancillary equation. The outcomes of this research will facilitate the determination of the optimal sediment transport water demand essential for preserving the main channel's integrity. This also helps in delineating specific bankfull discharges under varying water and sediment circumstances. Such insights are invaluable both theoretically and pragmatically for reservoir management, water resource distribution, and establishment of river ecological conservation strategies [28].

2. Materials and Methods

2.1. Study Area

The Yellow River characteristically manifests as a sandy and silty waterway; its main source of water and sediment is its middle reaches. In the latter half of the 20th century [23], the water flow and sediment transport of the Yellow River underwent notable transformation, precipitated largely by the dual effects of climate change and manmade interventions, such as water conservancy works, ecological construction projects, and regional socio-economic development. In the past century, the relationship between the Yellow River's water and sediment has transitioned from a discordant state during the natural period from 1919 to 1959, to a period of watershed management and erosion control through key projects from 1960 to 1999 [29]. These soil and water conservation efforts within the Yellow River Basin have led to a drastic reduction in water and sediment flowing into the lower reaches of the river. Further, the ongoing comprehensive management of the basin, spanning from 2000 to 2022, has had a profound impact on the water and sediment dynamics within the lower reaches [30]. Presently, the average annual sediment load reaching the lower stretches of the Yellow River is approximately 8×10^8 t, with the relationship between water and sediment reaching a state of coordination. A conspicuous downward trend is seen in both the water and sediment volumes of the Yellow River, with sediment changes outpacing those of the water. In the future, this decline in sediment volume is projected to continue.

The lower reaches of the Yellow River have the characteristics of wider and steeper sections upstream, transitioning into narrower and more gentle sections downstream. Erosion and sedimentation exhibit significant variations in the upper stretches, while the lower stretches remain relatively stable. Based on these traits, the lower Yellow River can be categorized into three different river types: wandering sections, transitional sections, and curved sections. Among them, Huayuankou Gaocun is a typical wandering-type river section (Figure 1). Given its substantial alterations in river types, the HYK-GC section meandering river segment was chosen for a targeted analysis and computation of sediment transport water demand.

2.2. Dataset

Since the 1950s, the Yellow River Water Conservancy Commission has constructed over 300 hydrological stations in the Yellow River Basin. After standardized calibration and compilation, datasets collected by each station are released as the 'Yellow River Hydrological Yearbook Data, serving as a valuable resource for engineering design and scientific research. For the purpose of this study, over 2800 sets of measured data were extracted from the 'Yellow River Hydrological Yearbook Data', spanning from 1960 to 2021. These data were collected from seven hydrological stations situated in the lower reaches of the Yellow River, namely Huayankou (HYK), Jiahetan (JHT), Gaocun (GC), Sunkou (SK), Aishan (AS), Luokou (LK), and Lijin (LJ). These datasets were applied to the analysis undertaken in this article (Table 1). The hydrological variables utilized include flow (Q), average flow depth (d), average flow velocity (v), slope (S), suspended sediment concentration (SSC), bed sediment diameter (D_{50}), suspended sediment diameter (d_{50}), sand settling velocity (ω), and Manning roughness (n) (Table 2). Among them, n is not measured directly, it is calculated through Manning's formula. N represents the number of data groups of each station. A summary in Table 1 reveals that the data used for validation spans a wide range. Thus, the use of these data to investigate the influencing factors of sediment transport water consumption and validate the calculation results ensures a comprehensive scope and accurate outcomes.

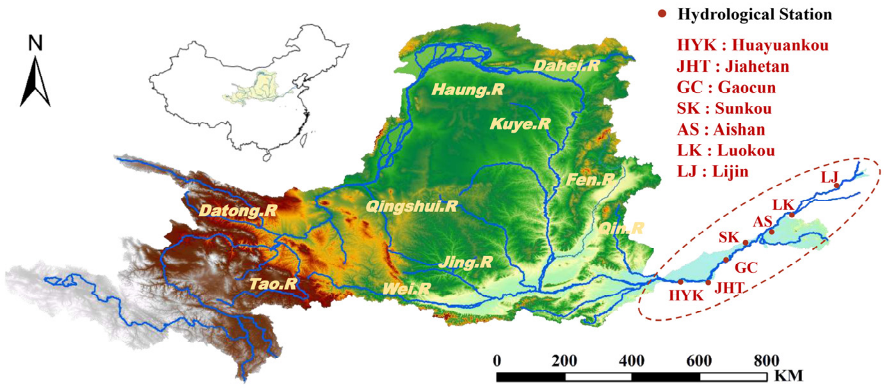

Figure 1. Map of Huanghe Basin and main hydrological stations. The location of the main hydrological research stations in the lower Yellow River are marked in the figure with red dots.

Table 1. The range of hydraulic variables in flow measurement in the study reaches.

Station	Q (m^3/s)	d (m)	v (m/s)	S (10^{-4})	SSC (kg·10^{-3})	D_{50} (mm)	n	ω (cm/s)	N
HYK	84–7750	0.53–5.2	0.5–3.33	0.4–9.4	0.232–465	0.012–0.37	0.0042–0.059	0.128–0.715	598
JHY	293–8400	0.53–6.1	0.44–2.87	0.12–8.7	0.253–456	0.029–0.244	0.0048–0.045	0.113–0.665	330
GC	60–7240	0.58–8	0.3–2.88	0.3–3.1	0.168–327	0.014–0.4	0.0036–0.05	0.143–0.655	619
SK	63–6670	0.50–4.7	0.36–2.9	0.12–6.0	0.055–209	0.010–0.323	0.0037–0.032	0.134–0.631	330
AS	52–9270	0.56–6.3	0.42–3.56	0.37–2.4	0.64–217	0.03–0.112	0.0048–0.027	0.107–0.702	492
LK	83–7500	0.96–11.3	0.41–2.76	0.33–6.1	0.58–188	0.035–0.218	0.0076–0.059	0.093–0.428	166
LJ	63–6280	0.52–4.99	0.35–2.78	0.4–2.1	0.157–211	0.031–0.248	0.0057–0.053	0.103–0.551	265

Table 2. The range of hydraulic variables in flow measurement in the study reaches.

Ws (10^8 t)	W (10^8 m^3)	v (m/s)	d (m)	w (m)	n	SSC (kg/m^3)
0.1	7.67	1.69	2.22	1065.66	0.0134	13.04
1	71.79	1.71	2.225	1056.94	0.0132	13.93
2	133.249	1.73	2.21	1047.47	0.0130	15.01
3	184.73	1.75	2.20	1037.91	0.0129	16.24
4	226.89	1.78	2.19	1028.27	0.0127	17.63
5	260.15	1.80	2.18	1018.54	0.0125	19.22
6	286.12	1.82	2.17	1010.05	0.0123	20.97
7	303.03	1.85	2.17	1000.14	0.0121	23.10
8	313.60	1.87	2.16	991.47	0.0120	25.51

2.3. Methods

The self-regulating behavior of alluvial channels can be directly explicated by three fundamental flow relationships: continuity, resistance, and sediment transport [31]. The water–sediment balance relationship refers to the relative equilibrium of sediment transport and the relative stability of the river channel that results from the riverbed's automatic adjustment [32]. Alluvial rivers' interaction between the riverbed and flow can shape a channel that facilitates a dynamic balance in water and sediment transport. The three basic equations that determine this equilibrium state—the continuity equation of flow, the conservation of momentum equation, and the resistance equation—contain four independent variables: river width, water depth, flow velocity, and slope. This makes the equation system theoretically unclosed. Three primary types of methods are used to construct the fourth equation that closes this system of equations. The first is the river stability equilibrium analysis method based on Newtonian mechanics, represented by Gary Parker [33,34]. The second method considers river equilibrium to reflect an extreme state, resulting in various extreme hypotheses [35,36]. However, these methods either involve complex solving processes or lack robust theoretical support. Thus, this article focuses on the third type of method. This involves finding suitable river dynamics equations as supplementary equations and constructing a closed equation system to address unknown quantities [37].

The conditions of erosion and sedimentation of the riverbed depend on the incoming water and sediment conditions as well as the sediment carrying capacity of the flow. This sediment carrying capacity is also related to the incoming water and sediment conditions and the riverbed's boundary conditions. Consequently, the riverbed morphology of alluvion rivers is a process of interaction and automatic adjustment between the flow and the boundary conditions of the riverbed. For highly adjustable alluvial channels, stable or relatively stable channel geometries represent a balance where the applied water and sediment loads can be transported without causing sedimentation or erosion [36]. The river channel's boundary morphology at this point can be described by introducing a hydraulic geometry relationship. Therefore, the closed equation group is composed of the continuity equation, moving bed resistance formula, and river phase formula. These can simultaneously solve the four hydraulic parameters of width, depth, slope, and velocity, and then, in conjunction with the sediment transport equation, solve the sediment transport water demand under a certain sediment condition.

Continuity equation:

$$Q_{bf} = v_{bf} w_{bf} d_{bf} \tag{1}$$

Manning formula:

$$v_{bf} = \frac{1}{n} R_{bf}{}^{\frac{2}{3}} S^{\frac{1}{2}} \tag{2}$$

Flow resistance equation:

$$n = n\left(v_{bf}, d_{bf}, S, D_{50}\right) \tag{3}$$

Hydraulic geometry relationship:

$$w_{bf} = w_{bf}\left(Q_{bf}\right),\ v_{bf} = v_{bf}\left(Q_{bf}\right),\ d_{bf} = d_{bf}\left(Q_{bf}\right),\ S = S\left(Q_{bf}\right) \tag{4}$$

Sediment transport equation:

$$SSC_* = SSC_*\left(v_{bf}, w_{bf}, d_{bf}, S, D_{50}, d_{50}; Q_{bf}\right) \tag{5}$$

where the subscript *bf* represents the bankfull condition, and R represents the hydraulic radius, which is usually replaced by the depth in wide and shallow river channels.

2.3.1. Resistance Formula of Moving Bed

In the aforementioned established equations, it is not only necessary to directly apply the continuity equation and Manning's equation but also to select suitable moving bed resistance equations, hydraulic geometry relationships, and sediment transport equations. Reliable prediction of flow resistance must reflect the changes in bed material particle size distribution and bed shape characteristics. This can be achieved by integrating single-value factors such as channel shape, flow conditions, and boundary conditions into a resistance calculation formula through the roughness coefficient.

Among the multitude of moving bed resistance formulas, Zhang's formula [38] (Equation (6)), established in 2019, incorporates the Froude number (Fr), a primary parameter that is related to, and substitutable with, other parameters that distinguish the motion state of sand waves [38,39]. It reflects the influence of changes in hydraulic sediment factors and the rise and fall of additional forms on the natural riverbed on flow friction characteristics. Furthermore, it accounts for the impact of sand skin friction through the median diameter D_{50} of the bed sand. This formula has a straightforward structure and has been verified as suitable for calculating roughness in the lower Yellow River. It is, therefore, believed that Equation (6) is the most suitable formula for calculating sediment transport water demand.

$$n = \frac{0.9{D_{50}}^{1/6}}{A_{50}(0.1 + 1.85Fr)} \tag{6}$$

where A_{50} is the reciprocal of the frictional resistance corresponding to D_{50}, which reflects the sand resistance and sand wave resistance, and can be taken as A_{50} = 19; D_{50} is the median particle size of the bed sand; Fr is the Froude number.

2.3.2. Sediment Transport Equation

The sediment carrying capacity of a flow is a comprehensive metric that reflects the flow's ability to carry sediment in a state of equilibrium between erosion and sedimentation in the riverbed [40,41]. Among the numerous sediment transport equations currently available, most are derived from shallow water experimental data in a laboratory environment, and the majority focus primarily on bed load transport [42]. For the Yellow River, however, suspended load sediment transport is the primary component of the total sediment transport within the river [43]. Hou et al. [44] selected 1115 groups of data that closely represented the equilibrium between erosion and deposition from measured hydrological data of the Yellow River. Using a variety of discriminant indicators and theoretical analyses, they tested ten sediment-carrying-capacity formulas applicable to the lower Yellow River. Ultimately, they concluded that the formula established by Zhang [45] (Equations (7)–(9)), which defines the suspended load sediment transport applicable to a hyper-concentrated flow from an energy conversion perspective, is the most effective for describing the sediment transport process of suspended load in the Yellow River.

$$SSC_* = 2.5\left[\frac{0.0022 + SSC_v}{\kappa\left(\frac{\rho_s - \rho_m}{\rho_m}\right)}\frac{v^3}{gd\omega_s}\ln\left(\frac{d}{6D_{50}}\right)\right]^{0.62} \tag{7}$$

where ρ_s is the density of sediment particles; ρ_m is the density of muddy water; ω_s is the average settling velocity of non-uniform sediment in clear water. This can reflect the impact of relative roughness on the sediment carrying capacity of the flow, improving the calculation accuracy and adaptability to different riverbed conditions. κ is the Karman constant of muddy water; SSC_* is the sediment carrying capacity of the water flow; SSC_v is the volume-specific sediment concentration. To calculate the sediment carrying capacity of flow using Equation (7), the influence of sediment concentration on the κ value and ω_s should be considered. The relationship between the two and sediment concentration is as follows:

$$\kappa = \kappa_0\left[1 - 4.2\sqrt{SSC_v}(0.365 - SSC_v)\right] \tag{8}$$

$$\omega_s = \omega_0(1 - 1.25SSC_v)\left(1 - \frac{SSC_v}{2.25\sqrt{d_{50}}}\right)^{3.5} \tag{9}$$

where κ_0 is the Karman constant of non-sediment flow, taken as 0.4; ω_0 is the average settling velocity of non-uniform sediment in clear water, cm/s; d_{50} is the diameter of suspended sediment, mm.

2.3.3. Hydraulic Geometry Relationship

Most river channels present stable or relatively stable hydraulic geometries that cannot be accounted for solely by continuity equations, resistance equations, and the basic flow relationships of sediment transport [46]. While numerous cross-sections with varying geometric shapes might satisfy specific flow and sediment transport criteria, observations of natural river channels suggest that they often maintain their unique shapes. In a state of equilibrium, there is a stable functional relationship between the shape of the main channel section and the flow of the bankfull beach in alluvial rivers, which is the correlation coefficient of the river along the way [26,47].

Zhang [45] believes that when calculating the overall average stability index of a river section, it is advisable to firmly grasp the factors that determine the stability of the river. $\varphi_{h_1} = \frac{D}{dS}$ should be used as the longitudinal stability coefficient, where D refers to the representative particle size of bed sand particles. The stable river width relationship $\varphi_{b_1} = \frac{Q^{0.5}}{S^{0.2}w}$ should be used as the lateral stability coefficient to construct a comprehensive index of riverbed stability:

$$Z_W = \frac{1}{S}\left[\frac{(\gamma_s - \gamma)}{\gamma}\frac{D_{50}}{d}\right]^{1/3}\left(\frac{d}{w}\right)^{2/3} \tag{10}$$

Upon evaluation, the formula in question demonstrates a comprehensive consideration of both longitudinal and transverse stability of the riverbed. It establishes clear boundaries for different river types and is amenable to both mountainous and plain rivers, as well as diverse riverbed compositions. Further, it is applicable to both prototype and model rivers. By using the measured data of the lower Yellow River from 2004 to 2020 to calculate the approximate river phase coefficient for erosion and sedimentation balance, it is observed that the HYK to GC section has been effectively regulated over the years. The comprehensive stability index has shown a marked increase from approximately 1.7 to between 3 and 4. However, it remains categorized as a wandering type of river channel with a value below the critical threshold of 5. Assuming the maintenance of the current river channel's balanced state without causing future trend shrinkage or expansion, the boundary characteristics of the current river channel can be integrated into the river correlation (Equation (10)). This serves as a pivotal formula for determining the average water depth.

2.3.4. Calculation Steps

Given specific conditions such as flat beach discharge, particle size, slope, and a comprehensive index of riverbed stability, it is possible to simultaneously determine four variables: river width (w), water depth (d), flow velocity (v), and roughness (n). This determination can be achieved using four equations: the continuity equation, the Manning formula, the roughness formula, and the comprehensive index of riverbed stability. The computational procedure is as follows: Firstly, we eliminate n by integrating Equations (2) and (6), assuming a water depth value d_0 from which the flow v can be calculated. Second, substituting v and d_0 into Equation (1) can derive w, so they are substituted into Equation (10) to obtain the corresponding Zw_0. Next, this Zw_0 is compared with the given Zw. If it is not equal, we change d_0 and repeat the trial until Zw_0 and Zw are equal. At this point, four key hydraulic parameters can be obtained through four equations. We substitute the obtained v and d into Equations (7)–(9) and assume a sediment concentration SSC_0 to obtain the corresponding sediment carrying capacity SSC_{*0}. If SSC_{*0} is not equal to SSC_0 at this point, we change SSC_0 and repeat the trial until they are equal to obtain the sediment concentration SSC at the equilibrium of erosion and sedimentation.

3. Results

3.1. Influencing Factors of Sediment Transport Water Demand

3.1.1. River Bed Morphology and Material Composition

- Median Particle Size of the Bed Sand D_{50}

The conditions of incoming water and sediment dictate the shifts in riverbed erosion and sedimentation [48]. When the sediment concentration of the water entering the river in its early stages is low, the riverbed experiences erosion, the composition of the bed sand coarsens, and the sediment carrying capacity of the flow decreases, leading to an increase in water demand for sediment transport. Conversely, when the sediment concentration of the incoming water in the early stages of the river is high, sedimentation transpires in the riverbed, refining the composition of the riverbed. Under these circumstances, the flow can transport more sediment, resulting in an increase in the sediment transport capacity of the flow and a decrease in the volume of water required for sediment transport [49]. On another note, the coarsening of bed sediment induces changes in riverbed resistance, which impacts flow velocity and, thus, the sediment carrying capacity of the flow. The measured data indicate that there will be no significant changes in the composition of the bed sediment, with average particle size variation not exceeding 50%. Nonetheless, its influence on the change in sediment carrying capacity can be significantly varied.

The collected data of median diameter D_{50} of bed sediment at each station in the lower Yellow River are divided into two periods, namely 1960–2000 and 2000–2021; the probability density distribution of the median diameter of bed sediment is graphically represented in Figure 2a. The diagram reveals that the distribution range of the median particle size of bed sediment in the lower Yellow River is wide, with the overall distribution being normal. Comparing the bed sediment diameters of the two periods before and after the operation of the Xiaolangdi Reservoir reveals that the bed sediment in the broad reach of the lower Yellow River has coarsened. According to statistical results, the average particle size of the river below Xiaolangdi Station has changed from 0.1 mm during 1992–2000 to 0.105 mm during 2006–2021. In fact, the variation in particle size of sediment at stations such as HYK Station is greater. This coarsening of bed sediment has increased bed resistance, resulting in a decrease in the sediment carrying capacity of the downstream stations for a given flow capacity. The amount of incoming sand also has an impact on the particle size of bed sand to some extent (Figure 2b), such as the D_{50} of GC-SK station decreasing with the increase of sediment transport load (Ws), which can be expressed by a fitting relationship. However, there is a significant difference in particle size among different stations, and values can be taken based on frequency distribution for downstream wandering sections.

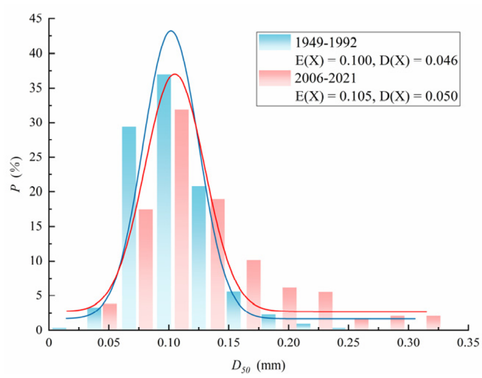

(**a**)

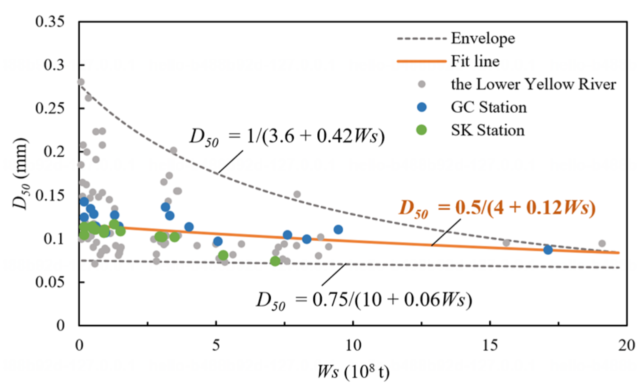

(**b**)

Figure 2. Statistical characteristics of bed sediment: (**a**) Probability density distribution map of D_{50} in the lower Yellow River. (**b**) Variation of D_{50} with Ws.

- Slope

The conditions of incoming water and variations in river erosion and sedimentation as induced by sediment inflow not only affect the thickness of bed sediment but also play a pivotal role in adjusting the bed surface gradient [20]. With a large volume of sediment, an initial accumulation of sediment is observed upstream. At this point, bed particles coarsen, leading to an increase in the roughness of the riverbed surface, which impedes the flow's ability to continue transporting sediment [21,22]. Consequently, the sediment transported to the downstream riverbed diminishes, resulting in an increase in the bed slope. On the other hand, when the volume of sediment is small, the flow initially erodes the upstream bed surface, transporting the dislodged sediment downstream, which in turn results in making the bed slope flatter. The author selected the measured data from HYK, JHT, and GC Stations in the lower Yellow River's wandering section from 1949 to 1992 and from 2006 to 2017 to create a probability density distribution of bed slopes (Figure 3a). The expected value of the bed slope in the wandering section prior to 2000 was 0.18‰. Due to the long-term reduction in sediment inflow and the improvement of river regulation in the lower Yellow River, the river slope in the wandering section has slightly decreased. Post-2000, the average slope in the wandering section reached 0.176 ‰. In the dataset, the measured slope primarily represents the water surface gradient, and it is assumed that the flow is uniform, using the water surface slope in place of the bed slope. Due to the large change amplitude of water surface gradient, the relationship between sediment inflow and slope is unclear. The measured values at GC-SK Station show a trend of increasing with the increase of *Ws* (Figure 3b), but for the entire downstream wandering river section, values can be taken according to frequency distribution.

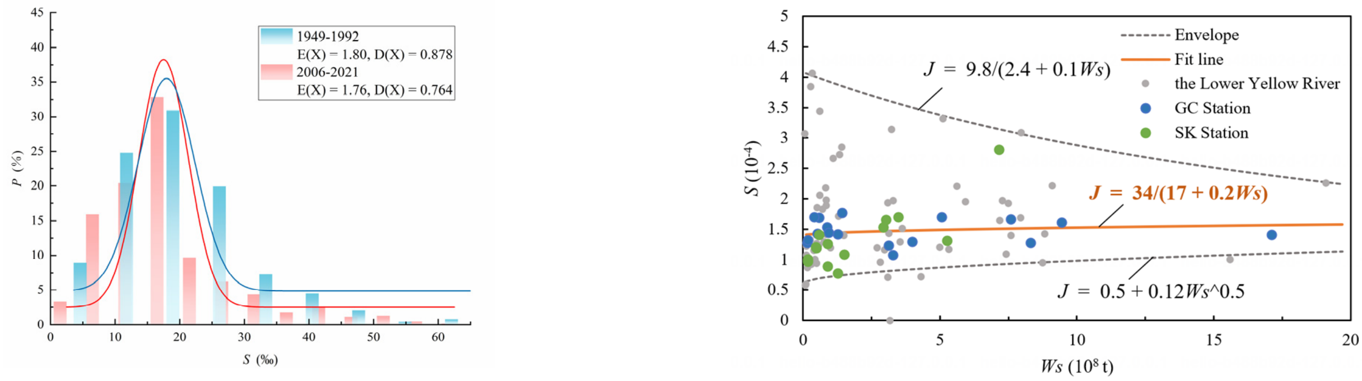

(**a**) (**b**)

Figure 3. Statistical characteristics of bed sediment: (**a**) Probability density distribution map of bed surface gradient in the lower Yellow River. (**b**) Variation of slope with *Ws*.

3.1.2. Incoming Water Conditions

- Sediment transport process under bed-making flow

Natural river channels undergo time-dependent changes in water and sediment processes. In the context of riverbed evolution analysis, engineering planning, and river regulation, it is often crucial to identify a representative flow, essentially encapsulating the cumulative effect of multi-year flow processes and playing a determinative role in riverbed shaping. This representative flow is commonly referred to as the 'bed-forming flow'. The bed-forming flow serves as a critical threshold delineating a river's transition from shaping the main channel to shaping the edge shoals. It also acts as a comprehensive parameter, encapsulating the flood and water volume of the sediment transport capacity of the main channel and the stable geometric form of the river channel, thereby reflecting the impact of human activities on the river's fundamental functions. At this flow level, the energy of the flow peaks and its role in shaping the riverbed are at their strongest [50]. Consequently, the water demand for sediment transport can be conceived as the corresponding volume of water necessary for the river to transport all incoming sediment at bankfull discharge, which is the point of maximum efficiency, without necessitating channel shrinkage.

A river's main channel in an equilibrium state is the product of long-term, self-dynamic adjustments. This can be equivalently conceptualized as the result of the continuous action of the bed-forming flow. Upstream sediment is efficiently transported in a saturated state of bankfull beach flow during flood periods. Consequently, the correlation between bankfull discharge and sediment transport water demand stems from the fact that continuous bankfull discharge shapes a balanced main channel of the river. Additionally, the water used in the efficient sediment transport process during flood periods—where the bankfull discharge and sediment concentration equate to the sediment carrying capacity of the flow—constitutes the sediment transport water demand. According to the latest research by scholars such as Hu and Zhang [51] on the bankfull discharge of the Yellow River, the short-term objective should be to shape and maintain the bankfull discharge of the Yellow River's lower reaches at 4000 m^3/s through river regulation. Over the long term, this flow rate should be maintained and essentially stabilized. The goal of restoring the cross-section of the main channel in the lower Yellow River is to achieve a bankfull beach discharge exceeding 4000 m^3/s.

- Total amount of incoming water and sediment

Alluvial river channels' erosion and sedimentation are influenced by numerous factors, including incoming water (encompassing flood peak form and volume), incoming sediment (encompassing grain size and sediment concentration), and river boundary conditions (including riverbed morphology and the extent of river control engineering, among others) [52]. However, when viewed from a long-term perspective, the predominant factors are the conditions of incoming water and sediment. The magnitude and duration of upstream inflow determine the extent of river erosion, which in turn influences the quantity of erosion and sediment transport [53]. Typically, erosion can only propagate throughout the lower reaches of the Yellow River below Xiaolangdi Station when the inflow exceeds 2500 m^3/s. Greater influxes of water lead to pronounced erosion, resulting in heightened sediment concentrations. Consequently, a smaller proportion of this water is required for sediment transport. In contrast, when incoming water volumes are reduced, erosion is less significant, necessitating a larger volume of water to facilitate sediment transport. Statistical analysis indicates that floodplain floods with a peak flow rate exceeding 6000 m^3/s contribute 93.8% of sedimentation during the peak period, while non-floodplain floods only account for 6.2%. Under certain incoming water and sediment conditions. When the flow discharge progressively approaches the bankfull discharge, the river's sediment carrying capacity reaches its maximum. During non-flood seasons, the erosion value above GC Station is relatively minor, but it prompts sedimentation below GC Station. Consequently, non-flood season sediment transport is uneconomical considering the quantity of sediment transport [54].

The relationship between the measured sediment transport and water consumption rate during the flood season from 1960 to 2020 and the volume of erosion and deposition are depicted in Figure 4. Observations indicate that when the sediment volume exceeds 15×10^8 m^3/t, if the sediment transport and water consumption rate is ≤ 20 m^3/t, sediment will accumulate in the downstream river channel. As the water consumption rate of sediment transport escalates from 20×10^8 m^3/t to 50×10^8 m^3/t, the riverbed state transitions from sedimentation to erosion. When the sand volume is less than 15×10^8 t, the water consumption rate of sediment transport increases from 40×10^8 m^3/t to 90×10^8 m^3/t, and the riverbed state shifts from sedimentation to erosion. However, under the same level of inflow and sediment conditions, different erosion and deposition situations can still arise, indicating that the state of riverbed erosion and deposition is not solely reliant on the combination of water and sediment conditions.

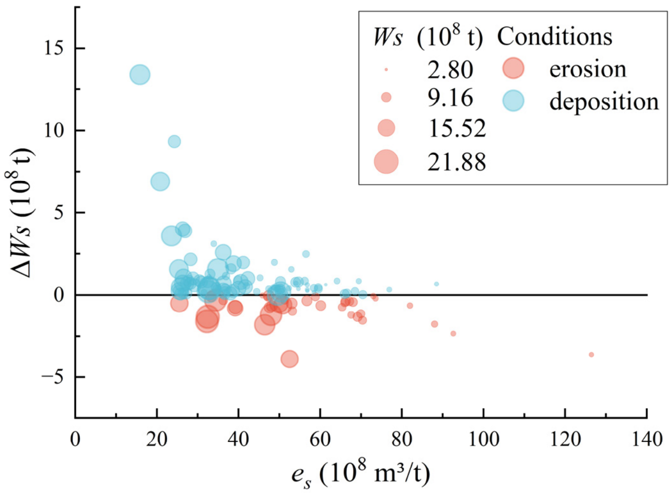

Figure 4. Measured water consumption for sediment transport during flood season, where e_s represents the water consumption rate of sediment transport, and ΔWs is the sedimentation amount of the riverbed; the positive values represent sedimentation, and the negative values represent erosion.

3.1.3. Conditions for Incoming Sand

- Sediment concentration

The quantity of sediment transport is also influenced by sediment concentration, for which there is an optimal range. Scholars [55] have found that the sediment carrying capacity of the lower reaches of the Yellow River is closely related to the sediment concentration at the upper station. The sediment transport in the river section exhibits a characteristic of 'more incoming and more discharging'. This characteristic is primarily due to changes in water and sediment properties caused by the quantity of sediment concentration, directly affecting the flow's sediment carrying capacity.

The relationship between water consumption for sediment transport and the erosion and sedimentation of downstream river channels during the flood season from 1960 to 2020 is depicted in Figure 5. It can be observed that when the water inflow is less than 300×10^8 m^3, sediment inflow is typically low, and the river is generally in a state of equilibrium between erosion and sedimentation. When the inflow is greater than 300×10^8 m^3 and the sediment concentration is about 15–25 kg/m^3, sediment transport can essentially maintain equilibrium. When the sediment concentration is in the range of 25–35 kg/m^3, as the inflow increases from 500×10^8 m^3 to 1000×10^8 m^3, the river transitions from slightly deposited to slightly eroded. If the sediment concentration is greater than 35 kg/m^3, the river channel is essentially in a siltation state.

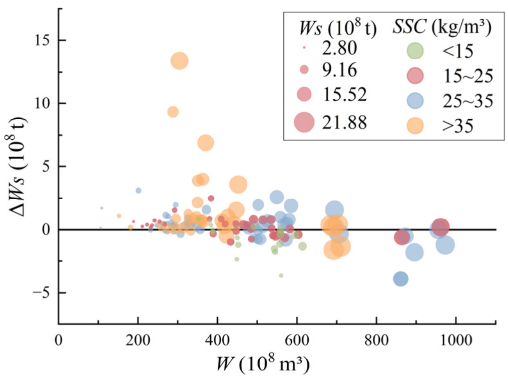

Figure 5. Relationship between water consumption for sediment transport with different levels of sand content and sediment erosion and deposition in downstream rivers.

According to the analysis results, it can be seen that the erosion and sedimentation situation in the lower reaches of the Yellow River is closely related to the changes in sediment concentration. Therefore, to obtain the most economical value of sediment transport volume, the sediment concentration should be within an appropriate threshold range.

- Median particle size of suspended sediment d_{50}

In conditions of high incoming sediment concentration, larger sediment particles tend to accumulate on the riverbed, resulting in a higher proportion of finer particles within the suspended sediment load [52,53]. Conversely, when the sediment load is small, the hydraulic processes tend to disturb and entrain more sediment from the riverbed, thereby increasing the proportion of coarser sediment particles within the suspended sediment. Thus, it is evident that the gradation of suspended sediment particles dynamically adjusts in response to changes in river erosion and sedimentation processes. A thorough analysis of the empirical data suggests that the gradation of suspended sediment is influenced by several factors, including the sediment concentration and the composition of bed sediment. It also exhibits a strong correlation with changes in hydraulic parameters, such as the sedimentation rate. For this analysis, 1522 sets of measured data from the lower Yellow River, spanning from 2006 to 2020, were utilized to plot the relationship between the median particle size of suspended sediment and the settling speed.

As depicted in Figure 6, the median particle size (d_{50}) of the suspended sediment load demonstrates a significant proportionality to the settling speed (ω). Consequently, the following empirical expression can be fitted to this observed relationship:

$$\omega = 5.9{d_{50}}^{0.85} \tag{11}$$

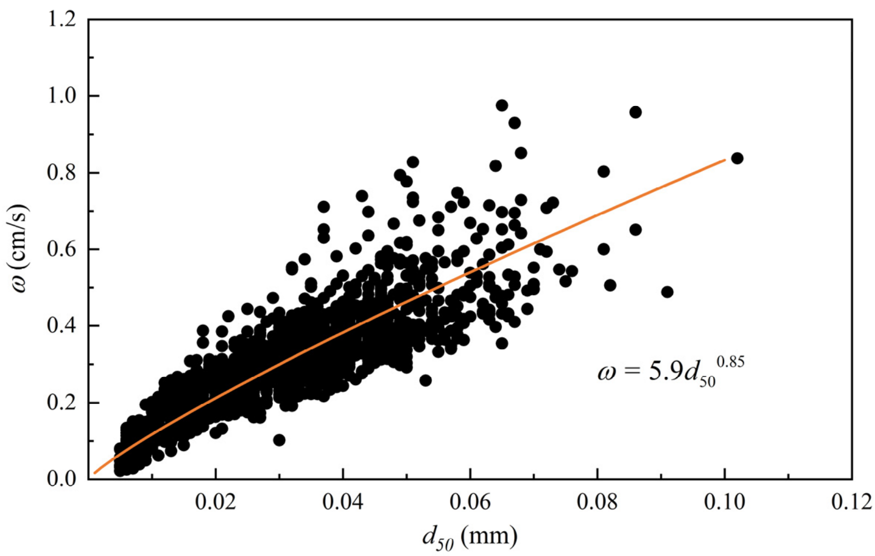

Figure 6. Relationship between d_{50} and ω of the lower Yellow River based on historical measurements.

However, there is also a pronounced correlation between suspended sediment and bed sediment runoff. The measured data of bed sediment and suspended sediment runoff from 18 stations in the main and tributaries of the Yellow River from 1960 to 2020 were selected and plotted in Figure 7. It can be found that there is a significant inverse relationship between d_{50} and D_{50}/d_{50}. When the suspended sediment diameter is taken as a smaller value, the corresponding D_{50}/d_{50} value range is larger, and as d_{50} increases, it gradually becomes a one-to-one correspondence with D_{50}/d_{50}. The average line can be approximately expressed as $D_{50}/d_{50} = 0.6/(0.03 + 4d_{50})$, and this curve can be used as the basis for determining the suspended sediment diameter under known bed sediment conditions.

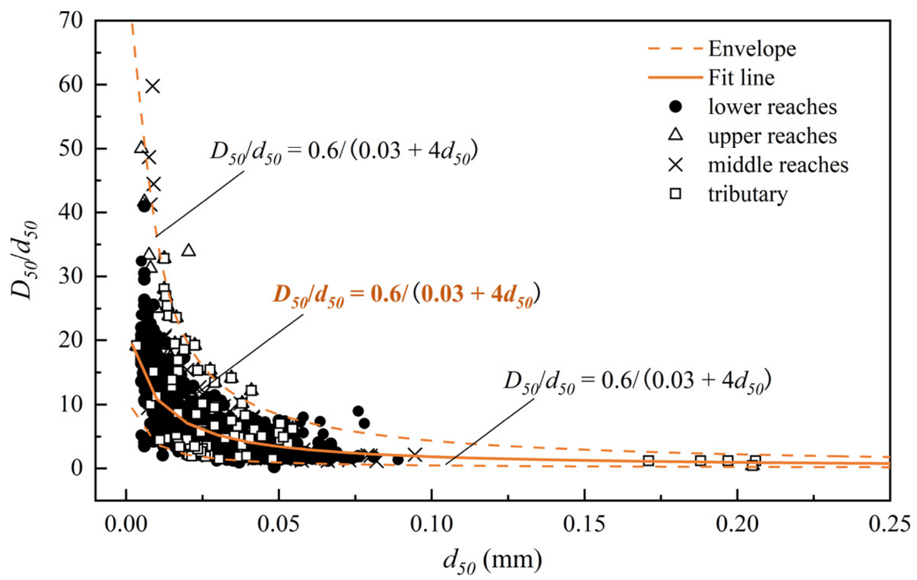

Figure 7. Relationship between d_{50}~D_{50}/d_{50} of the lower Yellow River based on historical measurements.

In summary, the hydraulic conveyance of sediment is influenced by a multitude of factors, which correlate with sediment concentration, discharge, fluvial sedimentation, and antecedent channel bed conditions. To comprehensively reflect the impact of hydrologic and sedimentary conditions as well as bed characteristics on the hydraulic demand for sediment transport, an approach for calculating sediment transport discharge during the flood season that reflects the equilibrium relationship of river channels should be proposed based on the principles of fluvial dynamics.

3.2. Calculation Results of Sediment Transport Water Demand

Under the given bankfull discharge Q_{bf}, the continuity equation (Equation (1)), the conservation of momentum equation (Equation (2)), the moving bed resistance equation (Equation (3)), and the relationship equation of the comprehensive stability index of the river bed (Equation (4)) are combined to solve the four unknowns of bankfull river width w_{bf}, water depth d_{bf}, flow velocity v_{bf}, and roughness n_{bf}. All variables are substituted into the sediment-carrying-capacity formula (Equations (7)–(9)), and the value of the sediment carrying capacity when the sediment concentration is in equilibrium is obtained through trial calculation. The sediment concentration at this point is the sediment concentration SSC_{bf} at the time of equilibrium sediment transport under the automatic adjustment of the river. Assuming that the total amount of sediment in a certain flood season is Ws, the water required to transport a certain amount of sediment can be calculated based on $W_{bf} = Ws/SSC_{bf}$, and this water amount is the water requirement for maintaining the balance of river erosion and sedimentation.

The recent sediment influx to the lower reaches of the Yellow River is about 8×10^8 t; this will gradually decrease to 0 over time with the continual decline of sediment influx. According to previous research, given a sediment volume density of 2.65 t/m^3 and an integral riverbed stability coefficient of four under a bankfull discharge of 4000 m^3/s in the lower Yellow River, when the incoming sediment volume changes from 8×10^8 m^3 to 0, the corresponding bed sediment diameter range is 0.1~0.105 mm, and the gradient range is 0.18~0.176‰. Furthermore, the suspended sediment diameter range is 0.015~0.03 mm, and the settling speed range is 0.14~0.26 cm/s. By substituting the changing parameter values into the above calculation steps, the relationship curve between sediment transport load (Ws) and amount of inflow (W) can be obtained.

Based on the obtained calculation results, the sediment transport characteristics of sediment-laden rivers can be observed. When the sediment inflow decreases from 8×10^8 t to 400×10^8 t, the corresponding sediment transport water increases from 31.7×10^8 m^3 to

22.8×10^8 m^3. This relationship indicates that as the sediment inflow decreases, the unit sediment transport water increases. The higher sediment concentration in the flow leads to a stronger ability of the flow to carry sediment, resulting in greater sediment transport efficiency. This reflects the sediment transport characteristics of sediment-laden rivers, which means that under the same flow conditions, when the upstream inflow has a high sediment concentration, the sediment transport capacity of each river section increases. Conversely, when the upstream inflow has a low sediment concentration, the sediment transport capacity of each river section decreases. This effect is particularly pronounced due to the presence of fine particles in the flow. To validate the accuracy of the calculation curve, data points from the main measuring stations in the lower Yellow River were plotted on the curve, representing inflow and outflow during the flood season from 1950 to 2020. The selected data points were those where the erosion and sedimentation amount of the river section reached a state of equilibrium. The amount of erosion and sedimentation in each river section was obtained by calculating the difference between the sediment inflow from a specific measuring station and the sediment inflow from adjacent downstream measuring stations. The purpose of plotting the measured data alongside the calculation curve was to assess whether the curve adequately reflects the relationship between the actual water volume of sediment transport and the sediment transport. As shown in Figure 8, the measured data generally align closely with the calculated value curve when the sediment concentration is high. However, as the sediment concentration decreases, deviations between the measured data and the curve become apparent.

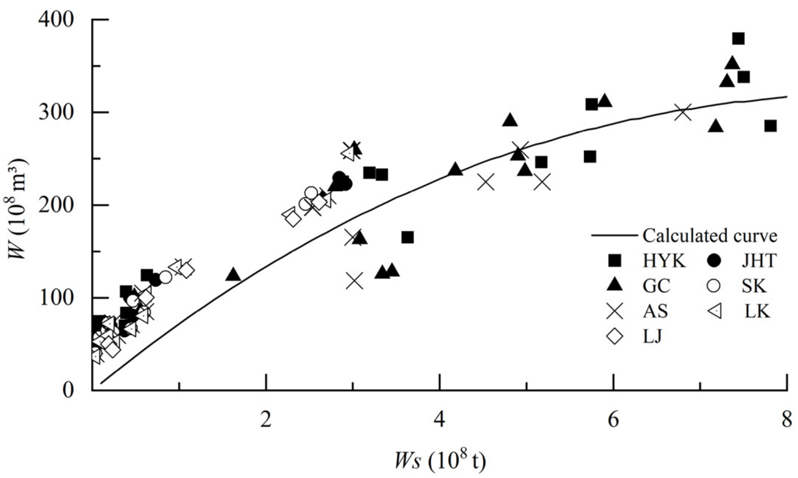

Figure 8. Curve of sediment transport water in the lower Yellow River.

4. Discussion

4.1. Calculation Reflecting the Overcurrent Capacity of the Main Tank

The determination of the river's bankfull discharge is influenced by various factors, including basin geological conditions and incoming water and sediment conditions. It is widely recognized by experts and scholars that bankfull discharge is not solely dependent on annual runoff processes but also influenced by previous runoff conditions. Additionally, bankfull discharge represents the maximum sediment carrying capacity of the river, which corresponds to the optimal sediment transport capacity. From a morphological perspective, bankfull flow signifies a critical point at which a river transitions from shaping the main channel to shaping the edge beach. It serves as a comprehensive parameter that reflects the flood and water volume of the sediment transport capacity of the main channel and the stable geometric shape of the river channel. As such, it can effectively capture the impacts of human activities on the fundamental functions of the river. Looking ahead, as sediment volume continues to decrease, the morphological development of the river will progress from a shallow and wide form to a narrower and deeper one. Once the main channel reaches equilibrium through erosion processes, its flow capacity will increase, resulting in an elevation of the bankfull discharge.

Based on the current regulated discharge of 4000 m^3/s in the lower Yellow River, this paper discusses changes in sediment transport discharge under several conditions of increased bankfull discharge. As sediment influx increases from 8 $\times$ 10^8 t to close to 0, (1) bankfull discharge remains unchanged at 4000 m^3/s; (2) discharge at Pingtan increases from 4000 m^3/s to 4300 m^3/s; (3) discharge at Pingtan increases from 4000 m^3/s to 4500 m^3/s; (4) discharge at Pingtan increases from 4000 m^3/s to 5000 m^3/s; (5) discharge at Pingtan increases from 4300 m^3/s to 4800 m^3/s; (6) bankfull discharge increases from 4500 m^3/s to 5000 m^3/s. In several cases, the bed slope decreases from 0.18‰ to 0.176‰, and the bed sand size increases from 0.1 mm to 0.105 mm.

We plotted the sediment influx and sediment transport discharge calculation results under six different bankfull discharges on the same graph (Figure 9). The results demonstrate that the sediment transport efficiency of flows under higher bankfull discharges is superior. When sediment influx is 8 $\times$ 10^8 t, transporting sediment at 4000 m^3/s requires 317 $\times$ 10^8 t of water, while transporting sediment at 4500 m^3/s requires 223 $\times$ 10^8 t of water. As bankfull discharge increases, the decrease in sediment transport discharge also increases, reaching a maximum difference when sediment influx is 4 $\times$ 10^8 t. For instance, sediment transport discharge at 4753 m^3/s is 150 $\times$ 10^8 m^3, reducing water consumption by 34.4% compared to using 4000 m^3/s for sediment transport. Subsequently, as sediment influx declines, the advantage of sediment transport efficiency under larger bankfull discharges is no longer significant. From the comparative calculation results, it can be seen that discharge has a regulatory effect on water consumption for sediment transport. A higher discharge will improve the sediment transport capacity of the flow, which is beneficial for concentrated sediment transport. Water consumption for sediment transport decreases with increasing discharge.

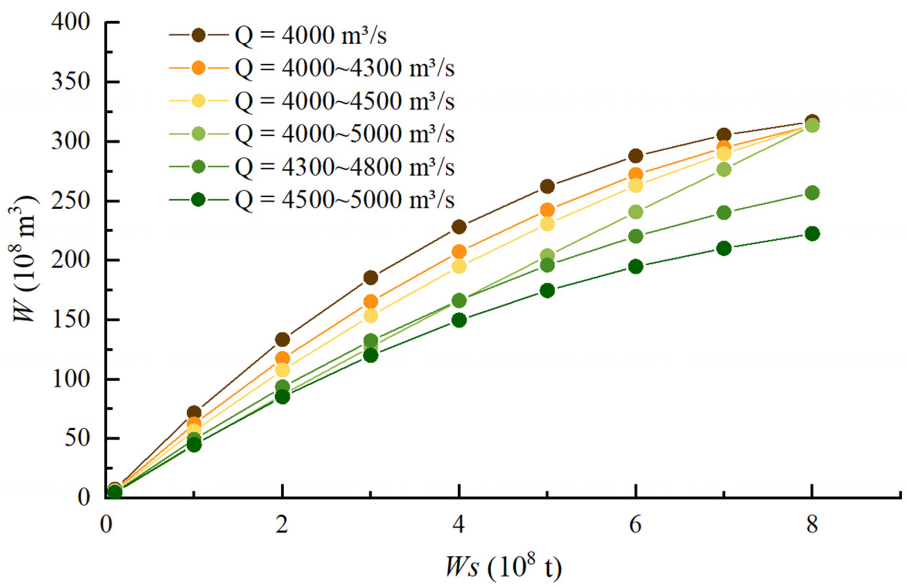

Figure 9. Comparison of water volume of sediment transport calculation results under different conditions of bankfull beach discharge variation.

4.2. Calculation Reflecting the Degree of River Regulation

The fluvial regime is a certain equilibrium relationship formed in alluvial river reaches under the long-term interaction between flow and moving bed sediment, which is suitable for the boundary conditions of the water, sediment, and channel bed. There is often a functional relationship between the relevant factors of this equilibrium form (such as depth, width, slope, etc.) and the characteristic physical quantities expressing the influx and sediment conditions (such as discharge, sediment concentration, particle size, etc.) as well as the geological conditions of the channel bed. Employing the integral channel bed stability index as a criterion to describe the river type and applying it to the calculation of sediment transport discharge can reflect the interaction between adjustment of the main channel form and the sediment transport capacity of the river. The braided reach from the HYK to the GC section needs further improvement in terms of integral channel bed stability indicators through continuous regulation. Under current conditions, the integral channel bed stability coefficient in the wide reach of the lower Yellow River is 4, which still belongs to the braided reach type. Zw = 5 is the critical value for transformation of the braided river type to the wandering river type in the lower Yellow River, indicating that the downstream braided reach has achieved the optimal level of regulation without changing the river type. Therefore, Zw = 5 can be considered the ideal expected value for regulation.

Given that Zw reflects the degree of constraint of river regulation on the river regime, changes in channel width-to-depth ratio, bed slope, and bed sediment size will all impact Zw, thereby reflecting the stability of the main channel form. To investigate the influence of different Zw values on sediment transport discharge in river channels, Q_{bf} = 4000 m^3/s was adopted as the target bankfull discharge to calculate sediment transport discharge under future river regulation scenarios. The following situations are discussed: as sediment influx increases from 8×10^8 t to close to 0, (1) Zw remains unchanged at 4; (2) Zw increases from 4 to 4.3; (3) Zw increases from 4 to 4.5; (4) Zw increases from 4 to 5; (5) Zw increases from 4.3 to 4.8; (6) Zw increases from 4.5 to 5. In several cases, bed slope decreases from 1.8‰ to 1.76‰, and bed sand size increases from 0.1 mm to 0.105 mm.

We plotted the sediment influx and sediment transport discharge calculation results under six Zw changes on the same graph (Figure 10). The results show that improving channel bed stability significantly reduces the sediment transport discharge required for the same sediment load. Compared with the river regulation situation where Zw = 4, the water required to transport 8×10^8 t sediment at Zw = 4.5 sharply decreases from about 317×10^8 m^3 to about 178×10^8 m^3. As Zw increases, the decrease in sediment transport discharge also increases, reaching a maximum difference when the sediment influx is 4×10^8 t. For instance, when Zw = 4.5, the sediment transport discharge is 139×10^8 m^3, reducing water consumption by 30% compared to the same conditions where Zw = 4 also transports 4×10^8 t sediment. Subsequently, incoming sand load declines. From the comparative calculation results, it can be seen that the stability of the channel form influences the sediment transport efficiency of the flow. The closer the channel form is to the stable state of the meandering type, the more beneficial for the river to transport sediment, thereby saving water for sediment transport.

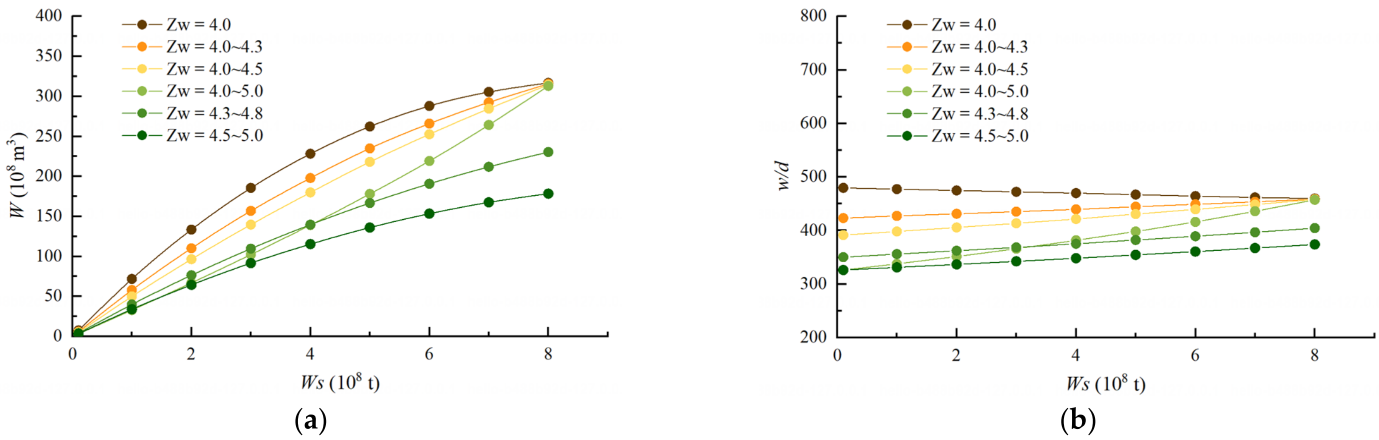

Figure 10. Comparison of water volume of sediment transport calculation results under different Zw variation conditions: (**a**) Ws~W; (**b**) Ws~w/d.

In reality, channel bed erosion leads to coarsening of bed sediment, an increase in D_{50}, a decrease in main channel width, an increase in depth, and an increase in Zw. To reflect the self-adjustment effect of the channel bed, it can also be observed from the calculation results that under conditions of constant bed slope and bed surface particle size, as sediment influx decreases and Zw increases, the channel width-to-depth ratio decreases, and the alluvial river morphology develops toward a narrow and deep direction. If different channel width conditions are given under the same conditions of bankfull discharge, bed sediment size, and bed slope, and the calculation results of sediment transport discharge are compared, it will be found that the smaller the channel width, the more stable the bed form, and the less the sediment transport discharge required under the same sediment influx conditions (Figure 11). As channel width decreases from 1000 m to 850 m, when sediment influx is 8×10^8 t, sediment transport discharge decreases from 317×10^8 m^3 to 170×10^8 m^3. At this point, Zw increases from 3.97 to 4.5. When sediment influx is 1×10^8 t, sediment transport discharge decreases from 61×10^8 m^3 to 40×10^8 m^3, at which point Zw increases from 4.18 to 4.74.

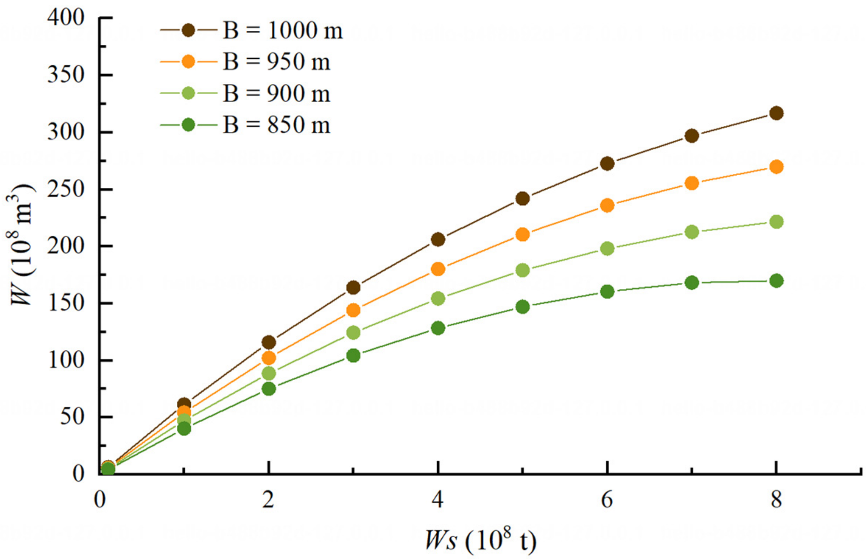

Figure 11. Calculation results of water volume of sediment transport under different river width conditions.

Therefore, given a specific bankfull discharge, the sediment transport rate of the main channel fluctuates with the adaptation of the river width. However, it is not beneficial for the river width to be minimized. Usually, an optimal main channel shape exists where the river width and water depth are optimized to produce maximum sediment transport efficiency. Consequently, investigating the optimal sediment transport cross-sectional shape of the ideal river channel and designing an efficient sediment transport channel following the principle of optimal main channel shape constitute the focal point of future research on water demand for sediment transport. This carries considerable significance for optimizing the layout of river control and navigation projects in the lower Yellow River, enhancing the sediment transport capacity of the river, and decreasing ecological water consumption.

4.3. Comparison with Other Studies

To enhance the validity and rigor of our findings, we juxtaposed our computed results with those documented in other studies. We chose six sediment transport volume calculation methods specifically tailored for the Yellow River and employed identical flow and sediment conditions for our computations. The sediment transport volumes corresponding to various sediment inflows are tabulated in Table 3. Moreover, the relationship between sediment inflow and sediment demand is graphically represented in Figure 12.

Table 3. Calculation results of water volume of sediment transport using different research methods.

Ws (10^8 t)	*W* (10^8 m^3)						
	This Paper	**Shen**	**Lu**	**Zhang**	**Wu**	**Yan**	**Shi**
0.1	7.67	87.73	85.42	96.17	62.55	46.8	3.3
1	71.79	96.11	131.07	115	104.53	148	32.96
2	133.249	105.42	181.79	135.92	122	209.3	65.91
3	184.73	114.73	232.52	156.84	133.55	256.34	98.87
4	226.89	124.04	283.24	177.76	142.4	296	131.82
5	260.15	133.35	333.96	198.68	149.67	330.94	164.78
6	286.12	142.66	384.68	219.6	155.88	362.52	197.74
7	303.03	151.97	435.4	240.52	161.33	391.57	230.69
8	313.60	161.28	486.12	261.44	166.21	418.61	263.65

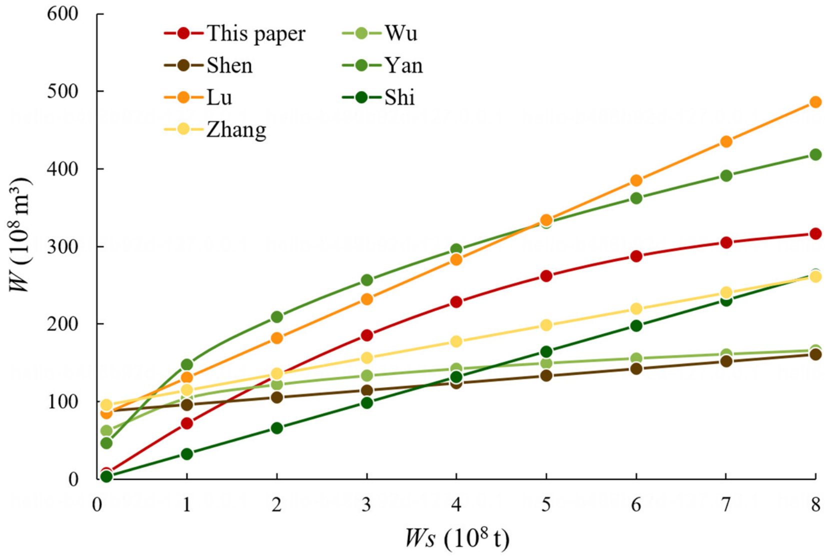

Figure 12. Calculation results of water volume of sediment transport using different research methods.

Based on the obtained results, the curves derived using the calculation methodologies of Shi, Shen, Zhang, and Lu are linear. This suggests that, irrespective of the varied water and sediment conditions, the per-unit sediment transport water volume remains constant, denoting uniform sediment transport efficiency. Notably, Lu's method exhibits the highest sediment transport efficiency. An analysis of prior data reveals that a river's sediment transport volume exhibits intricate dependencies on both incoming water and sediment conditions, as well as on the morphology of the riverbed. Given that natural river channels are perpetually in a state of erosion and sedimentation, their sediment transport capacities shift accordingly. Consequently, the per-unit sediment transport efficiency should not be static.

The computational approach of this study aligns with findings of Wu and Yan, with both highlighting an increasing trend in sediment transport efficiency as sediment inflow augments. Specifically, as sediment inflow grows, the sediment transport efficiency of Wu's model witnesses a pronounced surge, registering a water consumption of 142.4×10^8 m^3 at a sediment inflow of 4×10^8 t. In contrast, the increase in Yan's sediment transport efficiency is more tempered, with water consumption hitting 296×10^8 m^3 at the same sediment inflow. It is worth noting that the prospective total water inflow for the lower Yellow River might not achieve 300×10^8 m^3. Hence, dedicating all such inflow to ecological water usage for sediment transport is overly optimistic.

In summary, the sediment inflow to sediment discharge curve, determined via the method delineated in this article, occupies a median position amidst the other predicted curves. The computed values exhibit commendable concordance with actual measurements. The results underscore the intricate interplay between unit sediment discharge and hydraulic factors, positioning this method as a reliable computation mechanism for determining sediment discharge water demand that aptly captures the sediment transport dynamics of the lower Yellow River in contemporary scenarios.

5. Conclusions

The quantity of water utilized for sediment transport to maintain the equilibrium of river erosion and sedimentation forms an integral aspect of the ecological water in sandy rivers. Utilizing measured water and sediment data from the lower Yellow River spanning from 1960 to 2020, this study investigated the primary factors influencing sediment transport water demand. It also established a method for calculating sediment transport water demand based on the principles of fluvial dynamics. The findings suggest that the water demand for sediment transport correlates with the volume of incoming water, incoming sediment, and their ratio. For maximum economic efficiency in sediment transport, the sediment concentration should be within a specific threshold range. The water used for sediment transport within river channels is influenced by both the shape of the river boundary and the median particle size of the bed sediment, both of which are minimally affected by changes in the erosion and sedimentation state of the river channel. Based on the established closed equation system, the hydraulic parameters of flow velocity, water depth, river width, roughness, and sediment concentration during the balance of erosion and sedimentation are determined, reflecting the auto-adjustment effect of water and sediment. The flood-season sediment-transport water consumption to maintain the equilibrium of the main channel is obtained. The results indicate that as the sediment inflow decreases, the unit sediment-transport water volume increases. This suggests that when the sediment concentration is high, the flow's capacity to carry sediment is augmented, and the flow's efficiency in sediment transport is greater. When the sediment concentration in the upstream inflow diminishes, the sediment transport capacity of each river section along the route will decrease, primarily due to the high sediment concentration in the flow, especially the influence of fine particles. The water demand for sediment transport under equilibrium states decreases with the increase of the main channel flow capacity and the enhancement of river management. Hence, the construction of control and guidance projects to steer the river towards a more stable curved development is a key strategy to conserve ecological water in rivers.

Author Contributions: Conceptualization, L.H. and H.Z.; methodology, L.H. and H.Z.; software, L.H. and L.L.; validation, L.H.; formal analysis, L.H.; investigation, J.Z.; resources, L.H. and X.L.; data curation, L.H., J.Z. and X.L.; writing—original draft preparation, L.H. and L.L.; writing—review and editing, L.H. and L.L.; visualization, L.H.; supervision, H.Z.; project administration, L.H., H.Z. and L.L.; funding acquisition, H.Z. All authors have read and agreed to the published version of the manuscript.

Funding: This research was funded by the Key Projects in the National Science and Technology Support Program during the Thirteenth Five-Year Plan in China, 2016YFC0402500; National Natural Science Foundation, Youth Science Foundation of China, 52009145.

Data Availability Statement: Not applicable.

Acknowledgments: The authors thank the anonymous reviewers for their helpful comments and suggestions.

Conflicts of Interest: The authors declare that they have no known competing financial interest or personal relationships that could have appeared to influence the work reported in this paper.

References

1. Zhang, Y.F.; Wang, P.; Shen, G.Q. Characterizing and identifying bedforms in the wandering reach of the lower Yellow River. *Int. J. Sediment Res.* **2022**, *37*, 110–121. [CrossRef]

2. Wu, X.; Wang, H.J.; Bi, N.S.; Xu, J.P.; Nittrouer, J.A.; Yang, Z.S.; Lu, T.A.; Li, P.H. Impact of Artificial Floods on the Quantity and Grain Size of River-Borne Sediment: A Case Study of a Dam Regulation Scheme in the Yellow River Catchment. *Water Resour. Res.* **2017**, *57*, e2021WR029581. [CrossRef]
3. Pershin, I.M.; Papush, E.G.; Kukharova, T.V.; Utkin, V.A. Modeling of Distributed Control System for Network of Mineral Water Wells. *Water* **2023**, *15*, 2289. [CrossRef]
4. Martirosyan, K.V.; Chenyshev, A.B.; Martirosyan, A.V. Application of Bayes Networks in the Design of the Information System "Mineral Water Deposit". In Proceedings of the 2023 XXVI International Conference on Soft Computing and Measurements (SCM), Saint Petersburg, Russia, 24–26 May 2023; pp. 236–239. [CrossRef]
5. Ji, H.Y.; Chen, S.L.; Pan, S.Q. Fluvial sediment source to sink transfer at the Yellow River Delta: Quantifications, causes, and environmental impacts. *J. Hydrol.* **2022**, *608*, 127622. [CrossRef]
6. Yang, Y.C.; Liu, B.J. Reservoir ecological operation on sediment-laden river considering wetland protection. *Front. Environ. Sci.* **2023**, *11*, 1207032. [CrossRef]
7. Wang, H.; Wang, J.H.; Qin, D.Y.; Chen, C.Y.; Jiang, D.; Yao, Z.J. The Study on Water Resources Assessment and Subject System of Waterresources Study on Modern Times. *Adv. Earth Sci.* **2002**, *1*, 12–17.
8. Yang, Z.F. *Theory, Method, and Practice of Ecological Environmental Water Demand*; Science Press: Bäch, Switzerland, 2003; pp. 38–42.
9. Zhang, S.L.; Li, H.; Li, C.H.; Yi, Y.J.; Wang, X.; Liu, Q. Allocation of water resources in the lower Yellow river based on ecological footprint. *Front. Earth Sci.* **2023**, *10*, 1018980. [CrossRef]
10. Mosley, P.M. Analysis of the Effect of Changing Discharge on Channel Morphology and Instream Uses in a Braided River, Ohau River, New Zealand. *Water Resour. Res.* **1982**, *18*, 800–812. [CrossRef]
11. Li, X.F.; Yin, J.; Qiu, X.C. Effects of Seasonal Runoff Change on Eco-environmental Water Demand of Qingshui River Channel. *Bull. Soil Water Conserv.* **2022**, *42*, 23–28.
12. Wang, S.J.; Wang, X.M. Changes in Water and Sediment Processes in the Yellow River and Their Responses to Ecological Protection during the Last Six Decades. *Water* **2023**, *15*, 2285. [CrossRef]
13. Yi, Y.J.; Xu, J.X.; Song, J.; Liu, Q. Ecological water demand and discharge process calculation in the Yellow River Estuary. *Water Res. Prot.* **2022**, *38*, 133–140.
14. Fu, Y.C.; Leng, J.W.; Zhao, J.Y.; Na, Y.; Zou, Y.P.; Yu, B.J.; Fu, G.S.; Wu, W.Q. Quantitative Calculation and Optimized Applications of Ecological Flow based on Nature-based Solutions. *J. Hydrol.* **2021**, *598*, 126–216. [CrossRef]
15. Han, Q.; Tan, G.M.; Fu, X.; Yang, H.J.; Li, X. Calculation methods of river environmental flow and their applications. *Eng. J. Wuhan Univ.* **2018**, *51*, 189–197.
16. Chang, F.J.; Chen, L.; Chang, L.C. Optimizing the reservoir operating rule curves by genetic algorithms. *Hydrol. Process.* **2005**, *19*, 2277–2289. [CrossRef]
17. Wang, Z.Y.; Hu, C. Strategies for managing reservoir sedimentation. *Int. J. Sed. Res.* **2009**, *24*, 369–384. [CrossRef]
18. Yin, X.A.; Yang, Z.F.; Petts, G.E.; Kondolf, G.M. A reservoir operating method for riverine ecosystem protection, reservoir sedimentation control and water supply. *J. Hydro.* **2014**, *512*, 379–387. [CrossRef]
19. Yan, J.; Hu, C.H. Calculation and application of sediment-carrying water volume in the lower Yellow River. *J. Sed. Res.* **2004**, *4*, 25–32.
20. Wu, B.S.; Li, S.; Li, L.Y. Calculation methods of water demand for channel forming and sediment transport in the lower Yellow River. *J. Hydraul. Eng.* **2012**, *43*, 594–601.
21. Liu, X.Y.; Li, T.H.; Zhao, Y.A.; Jin, L.; Ni, J.R. Water demand for sediment transport in the lower Yellow River. *J. Basic Sci. Eng.* **2002**, *3*, 253–262.
22. Chen, M.; Xu, L.J.; Xing, C.P.; Xu, H.F.; Zhao, W.J. Analysis of the evolution trends and influential factors of bankfull discharge in the Lower Yellow River. *Sci. Rep.* **2022**, *12*, 19981.
23. Ma, Y.X.; Huang, H.Q. Controls of channel morphology and sediment concentration on flow resistance in a large sand-bed river: A case study of the lower Yellow River. *Geomorphology* **2016**, *264*, 132–146. [CrossRef]
24. Ni, J.R.; Liu, X.Y.; Li, T.H.; Zhao, Y.A.; Jin, L. Efficiency of sediment transport by flood and its control in the Lower Yellow River. *Sci. China Ser. E* **2004**, *47*, 173–185. [CrossRef]
25. Shen, G.Q.; Zhang, Y.F.; Zhang, M. Research on regulation indices of floods for high efficient sediment transport in the Lower Yellow River. *Yellow River* **2019**, *41*, 50–54.
26. Qin, C.; Wu, B.S.; Fu, X.D.; Wang, G. Progresses of hydraulic geometry study regarding the extension of spatiotemporal dimensions. *J. Sediment Res.* **2022**, *47*, 73–80.
27. Gregory, V.M.; Parker, G. Physical Basis for Quasi-universal relationships describing bankfull hydraulic geometry of sand-bed rivers. *J. Hydraul. Eng.* **2011**, *137*, 739–753.
28. Zhang, H.W.; Li, L.Q.; Peng, H.; Hou, L. Study on related problems of the Yellow River based on the goal of high-quality development of the basin. Water Res. *Hydropower Eng.* **2021**, *52*, 60–68.
29. Xu, J.X. Sediment Transferring Function of the Lower Yellow Riveras Influenced by Discharge and Sediment Load Conditions. *Sci. Geogr. Sin.* **2004**, *3*, 275–280.
30. Xia, J.Q.; Liu, X.; Zhang, X.L. Variation characteristics and formula of movable bed roughness for the Lower Yellow River. *Adv. Water Sci.* **2021**, *32*, 218–229.

31. Su, T.; Huang, H.Q.; Carling, P.A.; Yu, G.; Nanson, G.C. Channel-Form Adjustment of an Alluvial River Under Hydrodynamic and Eco-Geomorphologic Controls: Insights from Applying Equilibrium Theory Governing Alluvial Channel Flow. *Water Resour. Res.* **2021**, *57*, e2020WR029174. [CrossRef]
32. Huang, H.Q.; Chang, H.H.; Nanson, G.C. Minimum energy as the general form of critical flow and maximum flow efficiency and for explaining variations in river channel pattern. *Water Resour. Res.* **2004**, *40*, W04502. [CrossRef]
33. Parker, G. Self-formed straight rivers with equilibrium banks and mobile beds. Part l. The sand-silt river. *J. Fluid Mech.* **1978**, *89*, 109–125. [CrossRef]
34. Parker, G. Self-formed straight rivers with equilibrium banks and mobile beds, Part 2. The gravel river. *J. Fluid Mech.* **1978**, *89*, 127–146. [CrossRef]
35. Chang, H.H. Geometry of rivers in regime. *J. Hydraul. Div. ASCE* **1979**, *105*, 691–706. [CrossRef]
36. White, W.R.; Bettess, R.; Paris, E. Analytical approach to river regime. *J. Hydraul. Div. ASCE* **1982**, *108*, 1179–1193. [CrossRef]
37. Huang, H.Q.; Nanson, G.C. Hydraulic geometry and maximum flow efficiency as products of the principle of least action. *Earth Surf. Process. Landf.* **2000**, *25*, 1–16. [CrossRef]
38. Zhang, H.W.; Zhang, L.H.; Peng, H.; Cai, R.R. Research on cognition and calculation method of alluvial river roughness. *J. Hydraul. Eng.* **2020**, *51*, 774–787.
39. Zhang, H.W.; Zhao, L.J.; Cao, F.S. Research of the Cause of Formation of Wandering River Model and Its Changes. *Yellow River* **1996**, *10*, 11–15.
40. Albert, M.; Wu, B.S. Transport of sediment in large sand-bed rivers. *J. Hydraul. Res.* **2001**, *39*, 135–146.
41. Belikov, V.V.; Borisova, N.M.; Fedorova, T.A.; Petrovskaya, O.A.; Katolikov, V.M. On the Effect of the Froude Number and Hydromorphometric Parameters on Sediment Transport in Rivers. *Water Resour.* **2019**, *46*, S20–S28. [CrossRef]
42. Garcia, M.; Gary, P. Entrainment of Bed Sediment into Suspension. *J. Hydraul. Eng.* **1991**, *117*, 414–435. [CrossRef]
43. Tananaev, N.I. Applying regression analysis to calculating suspended sediment runoff: Specific features of the method. *Water Resour.* **2013**, *40*, 585–592. [CrossRef]
44. Hou, L.; Zhang, H.W.; Zhao, J.C.; Li, L.Q. Theoretical analysis and test of sediment carrying capacity formula. *J. Hydraul. Eng.* **2023**, *54*, 563–574+586.
45. Zhang, H.W.; Zhang, Q. Formula of sediment carrying capacity of the Yellow River. *Yellow River* **1992**, *11*, 7–9.
46. Konsoer, K.M.; Rhoads, B.L.; Langendoen, E.J.; Best, J.L.; Garcia, M.H. Spatial variability in bank resistance to erosion on a large meandering, mixed bedrock-alluvial river. *Geomorphology* **2016**, *252*, 80–97. [CrossRef]
47. Wright, S.; Parker, G. *Grain-Size Specific Suspended Sediment Transport and Flow Resistance in Large Sand-Bed Rivers*; Springer: Amsterdam, The Netherlands, 2003.
48. Parker, G.; Wilcock, P.R.; Paola, C.; Dietrich, W.E.; Pitlick, J. Quasi-universal relations for bankfull hydraulic geometry of single-thread gravel-bed rivers. *J. Geophys. Res.* **2007**, *112*, F04005.
49. Cheng, Y.F.; Xia, J.Q.; Zhou, M.R.; Deng, S.S.; Li, D.Y.; Li, Z.W.; Wan, Z.W. Recent variation in channel erosion efficiency of the Lower Yellow river with different channel patterns. *J. Hydrol.* **2022**, *610*, 127962. [CrossRef]
50. Wu, B.S.; Li, L.Y.; Zhang, Y.F. Water demand for keeping main-channel from shrinkage in the Lower Yellow River. *J. Hydraul. Eng.* **2011**, *42*, 1392–1397.
51. Hu, C.H.; Zhang, Z.H. The research of mechanism of constructing riverbed and index of flow and sediment of floodwater in the Lower Yellow River. *Sci. Sin.* **2015**, *45*, 1043–1051. [CrossRef]
52. Wang, Y.J.; Wu, B.S.; Zhong, D.Y. Adjustment in the main-channel geometry of the lower Yellow River before and after the operation of the Xiaolangdi Reservoir from 1986 to 2015. *J. Geogr. Sci.* **2020**, *30*, 468–486. [CrossRef]
53. van Scheltinga, R.C.T.; Coco, G.; Friedrich, H. Sediment Particle Velocity and Activity During Dune Migration. *Water Resour. Res.* **2021**, *57*, e2020WR029017. [CrossRef]
54. Shi, W.; Wang, G.Q. Review of studies on the water requirement for sediment transport of the lower Yellow River. *Adv. Water Sci.* **2003**, *14*, 118–123.
55. Lu, J.; Ma, L.M. Analysis of water demand for channel forming and sediment transport in the Upper Reaches of the Yellow River in Inner Mongolia. *Trans. Chin. Soc. Agric. Eng.* **2020**, *36*, 123–128.